Universität Rostock Traditio et Innovatio

Computational Science and Engineering

Computational Methods in Fluid Dynamics

Numerical Simulation of Incompressible Couette-Poiseuille Flow

Supervised by
Dipl.-Ing. Math. Ivan Shevchuk

Submitted by : Group 8

1.Atul Singh (216100191)
2.Onkar Jadhav (216100299)
3.Ranjith Arahatholalu Nandish (216100180)
4.Sudhanva Kusuma Chandrashekhara (216100181)
5.Ujjwal Verma (216100297)

Abstract

The goal in developing this simulation is to compare the velocity profiles obtained by running simulations between the komegaSST of simpleFoam solver with the experimental values obtained for couette poiseuille flow between two parallel walls. The Couette flow represents the flow between two parallel walls in which either one or both of them are defined moving. The simulation has been performed with Reynolds number 5000 and channel height 0.3 m indicating a limiting case between Couette Flow and Poiseuille type flow. This flow is modelled with SimpleFoam solver with mapping of velocity, turbulent kinetic energy , specific dissipation rate.The results are obtained at five stations for two different fvSchemes and three different mesh configurations to compare it with the experimental data.

Keywords : Couette poiseuille Flow, Mapped Boundary Condition, Upwind scheme, LinearUpwindV scheme.

Contents

List of Figures

List of Tables

1 Introduction

Couette Flow : Couette Flow is often used in illustrating the fluid motion between two parallel plates in which one of the plates is moving with velocity U and the other wall is fixed. Couette flow is shear or drag induced flow having zero pressure gradient in the fluid.

Poiseuille flow: Poiseuille flow is pressure driven flow between two stationary parallel plates. At the wall no slip condition is satisfied.[2]

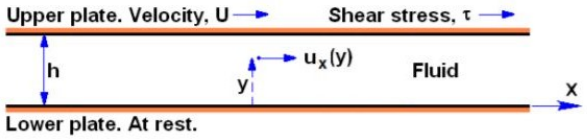

Figure 1: Couette Flow

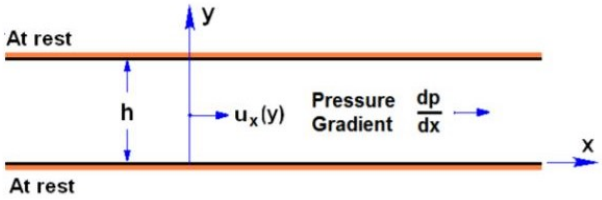

Figure 2: Poiseuille flow

2 Geometry and Mesh Generation

2.1 Geometry

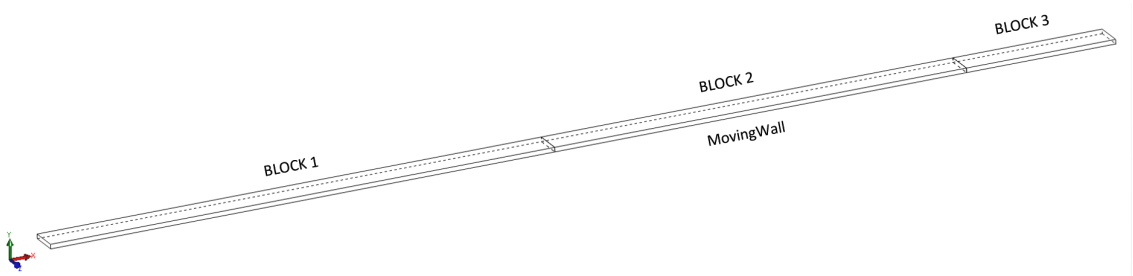

Figure 3: Geometry

The given geometry is a computational domain, orderly divided into 3 blocks with second block having moving wall as shown in the figure 3. Co-ordinates for the block are arranged in such a way that all blocks build the complete coherent geometry.
For this simulation 3 types of meshing are used i.e, Coarse, Medium and Fine meshing.

For Coarse Meshing

hex (0 1 2 3 4 5 6 7) (350 31 1) simpleGrading (1 ((0.2 0.3 10) (0.6 0.4 1) (0.2 0.3 0.1)) 1)
hex (1 8 9 2 5 11 10 6) (715 31 1) simpleGrading (1 ((0.2 0.3 10) (0.6 0.4 1) (0.2 0.3 0.1)) 1)
hex (8 12 13 9 11 15 14 10) (104 31 1) simpleGrading (1 ((0.2 0.3 10) (0.6 0.4 1) (0.2 0.3 0.1)) 1)

For Medium Meshing

hex (0 1 2 3 4 5 6 7) (490 44 1) simpleGrading (1 ((0.2 0.3 10) (0.6 0.4 1) (0.2 0.3 0.1)) 1)
hex (1 8 9 2 5 11 10 6) (1000 44 1) simpleGrading (1 ((0.2 0.3 10) (0.6 0.4 1) (0.2 0.3 0.1)) 1)
hex (8 12 13 9 11 15 14 10) (145 44 1) simpleGrading (1 ((0.2 0.3 10) (0.6 0.4 1) (0.2 0.3 0.1)) 1)

For Fine Meshing

hex (0 1 2 3 4 5 6 7) (686 62 1) simpleGrading (1 ((0.2 0.3 10) (0.6 0.4 1) (0.2 0.3 0.1)) 1)
hex (1 8 9 2 5 11 10 6) (1400 62 1) simpleGrading (1 ((0.2 0.3 10) (0.6 0.4 1) (0.2 0.3 0.1)) 1)
hex (8 12 13 9 11 15 14 10) (203 62 1) simpleGrading (1 ((0.2 0.3 10) (0.6 0.4 1) (0.2 0.3 0.1)) 1)

These blocks are defined as follows:
Vertex numbering : The first entry defines the shape of the block. Since the blocks are always hexahedral, the shape is always hex. Here, we follow the right-handed system.
Number of cells : The second entry defines the number of cells in each x,y and z-direction of the cells.
Cell expansion ratio : The third entry gives the ratio of expansion of cells in each direction. For mesh grading in y direction the cells are distributed in 20-60-20 ratio.

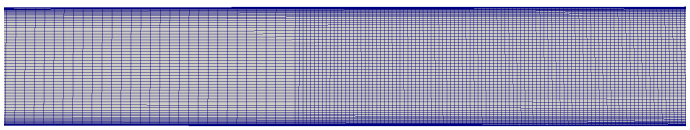

Figure 4: Mesh for Couette Poiseuille flow

2.2 Grid Generation

The flow near the wall is divided into four regions; Viscous Sub-layer, Buffer layer, Logarithmic region and Wake region. In regions close to solid walls the structure is dominated by shear due to wall friction and damping of turbulent velocity fluctuations perpendicular to the boundary. This results in a complex flow structure characterized by rapid changes in the mean and fluctuating velocity components concentrated within a very narrow region in the immediate vicinity of the wall.[3]

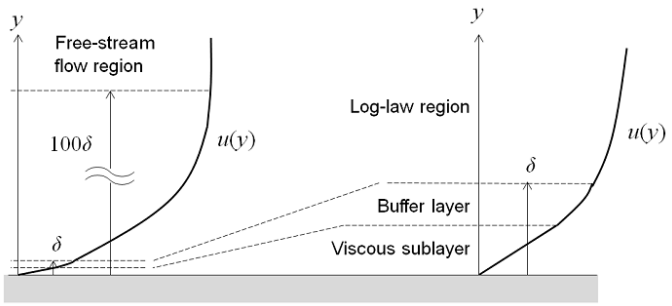

Figure 5: Four regimes of turbulent flow

So to capture the small eddies contained in these layers, the mesh should be fine enough to prevent the wall-adjacent cells from being placed in the buffer layer. For the simulation mesh refinement is done by the factor of 1.4 on the Coarse mesh.

3 Numerical calculations

3.1 Calculation for Initial Velocity (U_{in}):

$$R_e = \frac{U \times H}{\nu}$$

$$U = \frac{R_e \times \nu}{H} = \frac{5000 \times 3.75 \times 10^{-4}}{0.03}$$

$$\mathbf{U = 6.25}\ m/s$$

Where,
R_e = Reynolds number.
U = Maximum velocity of the object relative to the fluid (m/s).
H = Characteristic linear dimension (m).
ν = Kinematic viscosity (m^2/s).

3.2 Calculation of turbulence kinetic energy(k):

$$k = \frac{3}{2}(U \times I)^2 = \frac{3}{2}(6.25 \times 0.05)^2$$

$$\mathbf{k = 0.1465}\ m^2/s^2$$

Where,
R_e = Reynolds number.
U = Maximum velocity of the object relative to the fluid (m/s).
I = Turbulence fluctuation.

3.3 Calculation of Specific turbulence dissipation rate(ω):

$$\omega = C_u^{-\frac{1}{4}} \times \frac{\sqrt{k}}{L_T} = 0.09^{-\frac{1}{4}} \times \frac{\sqrt{0.1465}}{0.1 \times 0.03}$$

$$\omega\mathbf{=232.9361}\ 1/s$$

Where,
k = Turbulence kinetic energy(m^2/s^2).
L_T = Turbulent length(m) = $0.1 \times H$.

4 Boundary Condition

4.1 Inlet:

The inlet Boundary Condition for kOmegaSST is obtained by a recycling method. In the recycling method turbulent data are mapped from a plane positioned downstream of the inlet back to the inlet. However, the inlet and the mapping plane have to be placed far enough upstream of any disturbances in the flow.[4] In our case the offset distance specified is 0.845 m. The variables U, k and ω are mapped.

4.2 Outlet:

Velocity at the outlet is given by Neumann's boundary condition.[5] At the outlet of the model, the typical boundary condition for pressure is fixed static pressure.

$$\frac{\partial U}{\partial n} = 0, p = o, \frac{\partial k}{\partial n} = 0, \frac{\partial \omega}{\partial n} = 0$$

4.3 At fixed walls:

No slip condition is specified which means velocities in these directions are zero. No-slip conditions- k: kLowReWallFunction, ω : omegaWallFunction ν_t : nutLowReWallFunction.

4.4 At moving wall:

Velocity of the moving wall is assumed as 1.2 times inlet velocity as referenced from the experimental data.[1] i.e, $U = (U_w, 0, 0)^T$
where,
$U_w = 1.2 \times U_{in} = 7.5m/s$,
$\frac{\partial p}{\partial n} = 0$,
k: kLowReWallFunction,
ω : omegaWallFunction ,
ν_t : nutLowReWallFunction.

4.5 LowReWallFunctions:

Wall functions based on the log-law are inaccurate in Low Reynolds number flows. kLowReWallFunction; nutLowReWallFunction ,are used as they provide a turbulence kinetic energy wall function condition for low- Reynolds number turbulent flow cases.[6] Low Reynolds number modifications to the models can be incorporated to add the effects of molecular viscosity to the diffusion terms.[7]

5 Fv Schemes

5.1 Upwind scheme

- The upwind differencing scheme takes flow direction in account when determining the value at a cell face which is a major inadequacy of the central differencing scheme.[8]
- It is a first-order bounded scheme.
- Discretization scheme for convective term is changed to upwind in openFOAM.
- Upwind-biased interface values are given as,
  For a>0,
  $$I_c \approx a\frac{u_i - u_{i-1}}{\triangle x}$$
  For a<0,
  $$I_c \approx a\frac{u_{i+1} - u_i}{\triangle x}$$

5.2 Linear Upwind 'V' Scheme

- Linear Upwind is a second order unbounded scheme, that requires discretisation of the velocity gradient to be specified.
- Discretization scheme for convective term is changed to 'V'-scheme namely linear Upwind V grad(U) in openFOAM.
- 'V'-schemes are designed for vector fields. The 'V'-scheme calculates single limiters based on the direction of most rapidly changing gradient, resulting in the strongest limiter being calculated which is most stable but less accurate.[9]

6 Mathematical Model

6.1 k- ω SST Model

The SST k-ω turbulence model is a two-equation eddy-viscosity model. In which k is a turbulence kinetic energy and omega is the specific rate of diffusion. k-ω SST model shows its better results in adverse pressure gradients and separating flow.[10] Kinematic Eddy Viscosity,

$$\nu_T = \frac{a_1 k}{\max(a_1\omega, SF_2)}$$

Turbulence Kinetic Energy,

$$\frac{\partial k}{\partial t} + U_j\frac{\partial k}{\partial x_j} = P_k - \beta^* k\omega + \frac{\partial}{\partial x_j}\left[(\nu + \sigma_k\nu_T)\frac{\partial k}{\partial x_j}\right]$$

Specific Dissipation Rate,

$$\frac{\partial \omega}{\partial t} + U_j\frac{\partial \omega}{\partial x_j} = \alpha S^2 - \beta\omega^2 + \frac{\partial}{\partial x_j}\left[(\nu + \sigma_\omega\nu_T)\frac{\partial \omega}{\partial x_j}\right] + 2(1-F_1)\sigma_{\omega 2}\frac{1}{\omega}\frac{\partial k}{\partial x_i}\frac{\partial \omega}{\partial x_i}$$

Closure Coefficients and Auxilary Relations,

$$F_2 = \tanh\left[\left[\max\left(\frac{2\sqrt{k}}{\beta^*\omega y}, \frac{500\nu}{y^2\omega}\right)\right]^2\right]$$

$$P_k = \min\left(\tau_{ij}\frac{\partial U_i}{\partial x_j}, 10\beta^* k\omega\right)$$

$$F_1 = \tanh\left\{\left\{\min\left[\max\left(\frac{\sqrt{k}}{\beta^*\omega y}, \frac{500\nu}{y^2\omega}\right), \frac{4\sigma_{\omega 2}k}{CD_{k\omega}y^2}\right]\right\}^4\right\}$$

$$CD_{k\omega} = \max\left(2\rho\sigma_{\omega 2}\frac{1}{\omega}\frac{\partial k}{\partial x_i}\frac{\partial \omega}{\partial x_i}, 10^{-10}\right)$$

$$\phi = \phi_1 F_1 + \phi_2(1 - F_1)$$

$$\alpha_1 = \frac{5}{9}, \alpha_2 = 0.44$$

$$\beta_1 = \frac{3}{40}, \beta_2 = 0.0828$$

$$\beta^* = \frac{9}{100}$$

$$\sigma_{k1} = 0.85, \sigma_{k2} = 1$$

$$\sigma_{\omega 1} = 0.5, \sigma_{\omega 2} = 0.856$$

7 Modeling and Discretization error

7.1 Modeling Error

Uncertainty of formulations and simplification of model leads to physical errors. Errors are concerned with the choice of governing equations model led according to their properties.
Sources of uncertainty in physical models may be through

1)Phenomena is not thoroughly understood
2)Model parameters are known with some uncertainty
3)Models are simplified, introducing some uncertainty
4)Experimental confirmation is impossible.

These are examined with validating studies that focus on certain models.[11]

7.2 Discretization error

In practical CFD simulations the discretization errors is dominant than the modeling error. The temporal and spatial derivatives of flow variables that appear in the equations are approximated on the chosen time and space mesh. In theory, the errors can be reduced by progressively reducing the time and space step on the cost of increasing memory and computing time.[11]

8 Results

8.1 Residuals, yPlus and Convergence

The difference between the left and right hand sides of the discretized momentum equation at every velocity node is called the momentum residual. If the iteration sequence is convergent this residual should decrease to show an improving balance between the computed velocity and pressure fields.
Ideally, we would like to stop the iteration process when mass and momentum are exactly balanced in the discretized pressure correction and momentum equations.Our aim is to truncate the iterative sequence when we are sufficiently close to exact balance.[12]
The below table has the values of relaxation factor ,tolerance and residual control for Pressure and velocity fields.

FV Scheme	Mesh	Iteration	Residual	yPlus
Upwind	coarse	3745	8.2876e-07	0.85376
	medium	5218	7.09532e-07	0.605382
	fine	7803	5.77502e-07	0.418274
Linear Upwind	coarse	3835	8.41875e-07	0.85285
	medium	5211	7.31592e-07	0.604581
	fine	7829	8.98831e-07	0.418075

Table 1: Residuals, yPlus and convergence

Fields	Residual control	Tolerance	Relaxation Factor
P	1e-05	P=1e-06	0.4
U	1e-05	U=1e-05	0.3
k-Omega	1e-03		

Table 2: Residual control

8.2 Comparison of Experimental and Simulated Results

8.2.1 Upwind Scheme

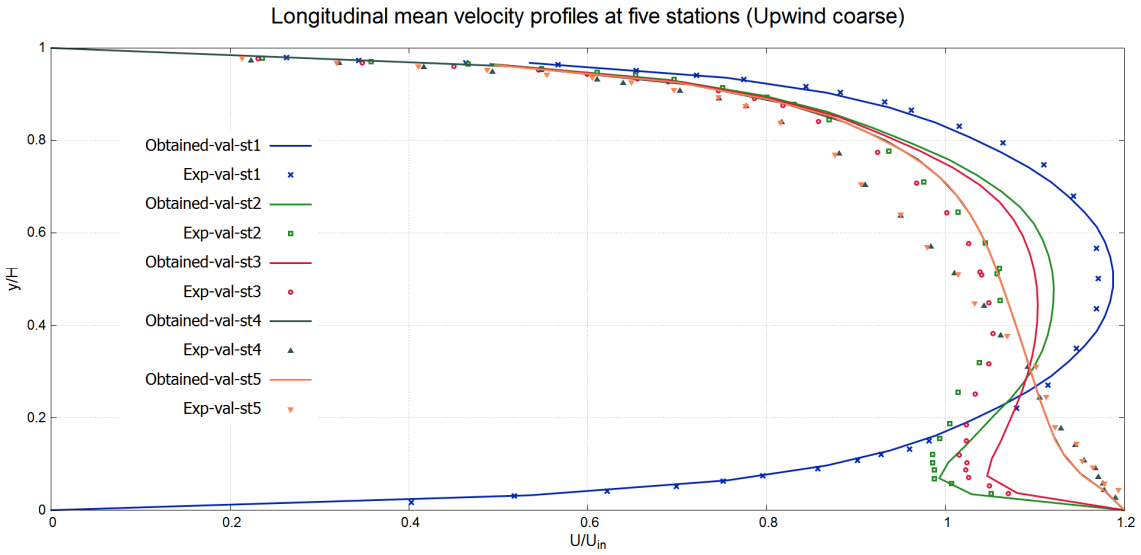

Figure 6: Longitudinal mean velocity profies at five stations (Upwind coarse)

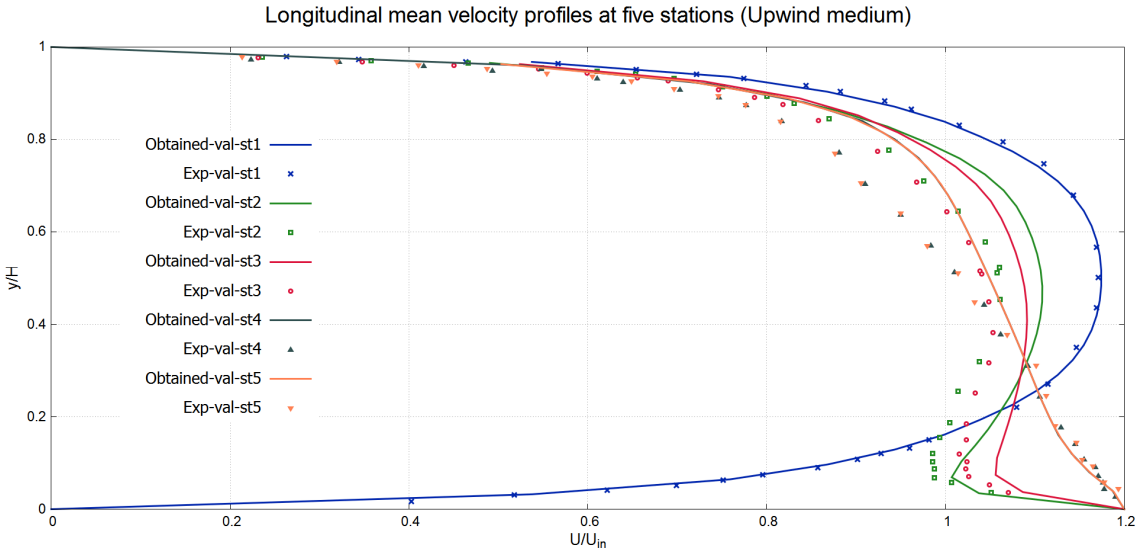

Figure 7: Longitudinal mean velocity profies at five stations (Upwind Medium)

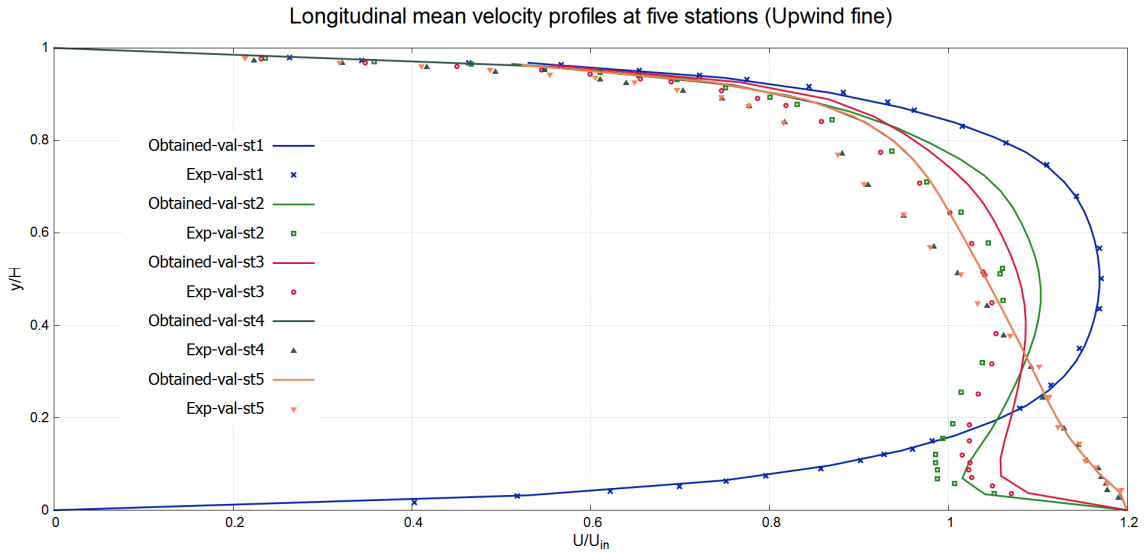

Figure 8: Longitudinal mean velocity profies at five stations (Upwind Fine)

8.2.2 Linear Upwind

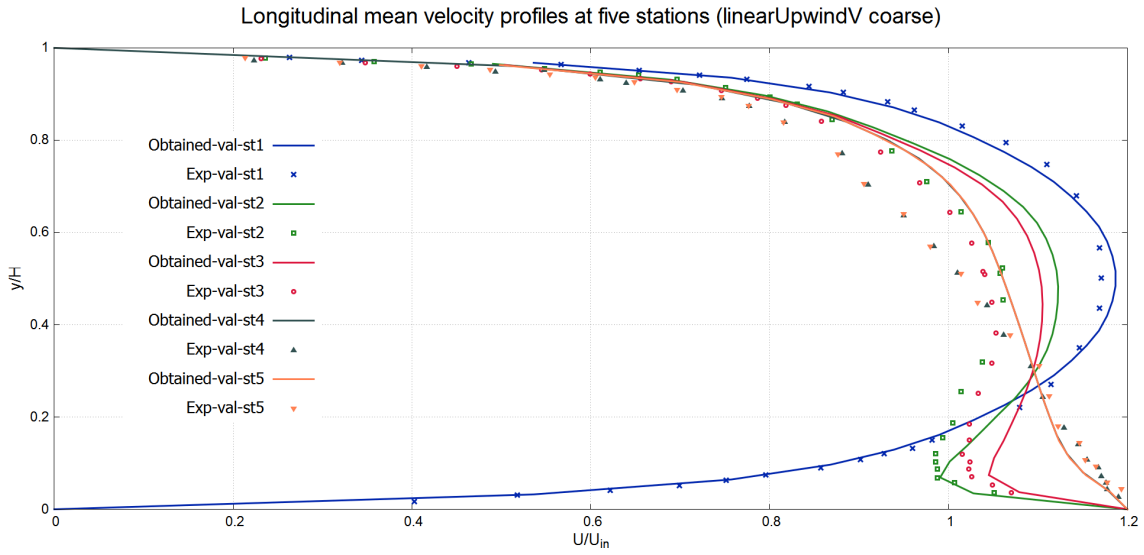

Figure 9: Longitudinal mean velocity profies at five stations (LinearUpwindV coarse)

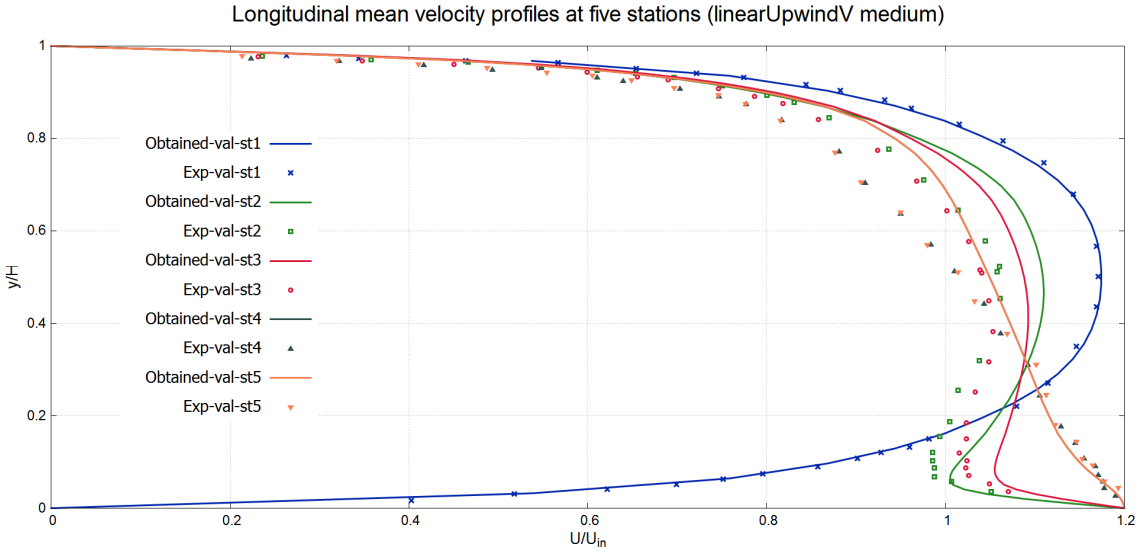

Figure 10: Longitudinal mean velocity profies at five stations (LinearUpwindV medium)

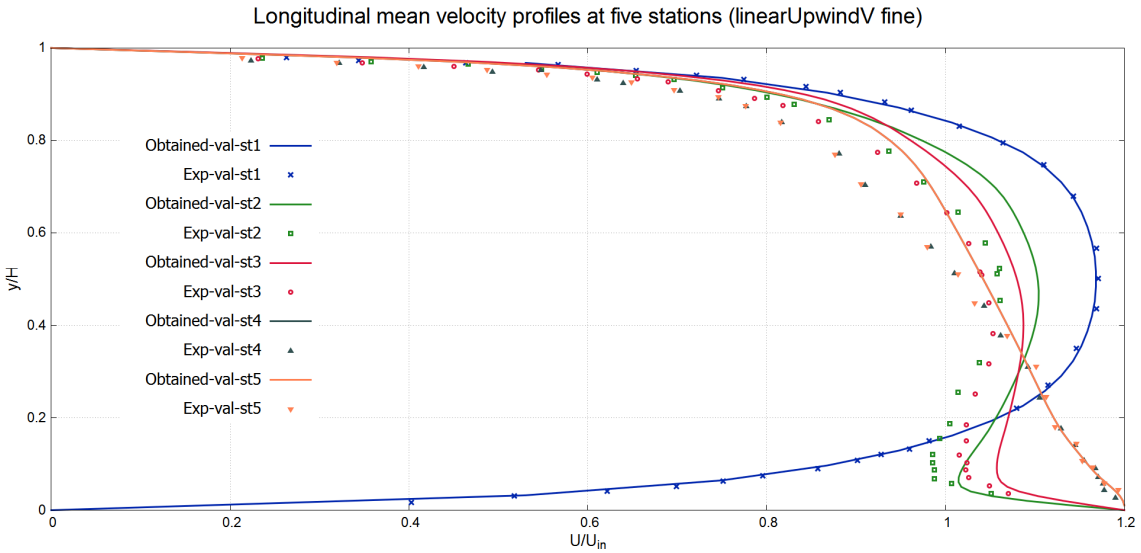

Figure 11: Longitudinal mean velocity profies at five stations (LinearUpwindV fine)

9 Discussion

This section highlights some of the general characteristics of the flow observed in earlier chapters. The wall velocity U_w has been set at 7.5 m/s and U_{in} is calculated as 6.25 m/s from the Reynolds number (Re = 5000) and channel height (H=0.03 m)[1].
Observations are made at five different stations, four of them are in the second block having moving wall and one of them in the first block with fixed wall. Comparison between the results of k-ωSST model and the experimental setup for couette poiseuille flow has been presented.
As the flow advances from left to right with positive pressure gradient it leads to a fully developed flow at station 1 which can be observed in Figure 10.
The results, as observed from the Figures 5 to 10, compares favourably for the first station. It can also be observed that with increase in fineness of the mesh the nature of the obtained profiles are tending towards the experimentally obtained result. Thus it can be inferred that the large discretization errors is reduced considerably. Some improvements however, can be made to enhance the prediction by specifying grid spacing in both direction of the mesh.
Upwind is a first order bounded scheme and the Linear UpwindV scheme is a second order unbounded scheme. Upwind scheme is also more stable scheme hence the simulation performed using upwind scheme has to converge faster and the same has been observed from the Table 1. [13]
The k-ω model SST can be used for Low-Re number turbulent flow and it also gives better results for the wall bounded flow which can be evidenced from the Figures 5 to 10 as the simulated and experimental results are matching. [14]

10 Conclusion

- Increasing the mesh resolution decreases the discretization error, which yields the obtained results close to the experimental ones.
- With increase in mesh resolution the deviation between the obtained results and that of experimental, decreases as compared to the deviation between two different schemes with the experimental result, which concludes that modelling error is less than discretization error.
- Linear Upwind scheme gives better result compared to Upwind scheme.
- As the upwind scheme is of first order it converges earlier than linear upwind and the same is evident from the Table 1.

11 Reference

References

[1] Corenflos, K., Rida, S., Monnier, J.C, Dupont, P., Dang Tran, K. and Stanislas M. *Experimental and numerical study of a plane Couette-Poiseuille flow as a test case for turbulence modeling.* Elsevier Series in Thermal and Fluid Sciences

[2] Brennen, Christopher E. *Index - An Internet Book On Fluid Dynamics.* Brennen.caltech.edu. updated 6/10/06.

[3] *Which Turbulence Model Should I Choose For My CFD Application?* COMSOL Multiphysics©. N.p., 2017. Web. Feb. 2017.

[4] Jorgensen, Nina Gall. *Implementation Of A Turbulent Inflow Boundary Condition For LES Based On A Vortex Method.* A COURSE AT CHALMERS UNIVERISTY OF TECHNOLOGY, 2012. Print.

[5] Cheng, Alexander H.-D. and Daisy T. Cheng *Heritage And Early History Of The Boundary Element Method* Engineering Analysis with Boundary Elements 29.3 (2005): 268-302.

[6] *Openfoam: Wall Functions* Openfoam.com

[7] *Low-Re Resolved Boundary Layers – CFD-Wiki, The Free CFD Reference* Cfd-online.com.

[8] Patankar, Suhas V. *Numerical Heat Transfer And Fluid Flow* 1st ed. [U.S.]: Hemisphere Pub., 1980. print.

[9] Greenshields, Christopher J. *OpenFOAM User Guide. 3rd ed.* OpenFOAM Foundation Ltd., 2015. Print.

[10] Prof. Dr.-Ing. habil. Nikolai Kornev and Prof. Dr.-Ing. habil. Irina Cherunova *Lectures on computational fluid dynamics and heat transfer with applications to human thermo-dynamics* 1st ed. 2014. print.

[11] Grc.nasa.gov. *Uncertainty And Error In CFD Simulations* jul 17 2008.

[12] Versteeg, Henk K and W Malalasekera. *An Introduction To Computational Fluid Dynamics.* 2nd ed. Harlow: Pearson/Prentice Hall, 2010. Print.

[13] Strang, Gilbert. *Linear Algebra And Its Applications* 1st ed. Belmont [etc.]: Thomson Brooks/Cole, 2006. Print.

[14] *SST K-Omega Model – CFD-Wiki, The Free CFD Reference* Cfd-online.com.